MAUSAM, **74**, 2 (April, 2023), 467-482

MAUSAM

DOI : https://doi.org/10.54302/mausam.v74i2.5983
Homepage: https://mausamjournal.imd.gov.in/index.php/MAUSAM

UDC No. 551.577.37 : 551.588.1

Impact of genesis conditions on regional simulations of extreme rainfall : A convection parameterization sensitivity study

MANPREET KAUR*, SUSMITHA JOSEPH, R. PHANI, A. K. SAHAI, A. DEY and R. MANDAL

Indian Institute of Tropical Meteorology, Ministry of Earth Sciences, Pune – 411 008, India

**Department of Atmospheric and Space Sciences, Savitribai Phule Pune University, Pune – 411 007, India*

e mail : manpreet.phy@gmail.com

सार – भौतिक प्राचलीकरण में अनुमानित और सरलीकृत वास्तविक-वायुमंडलीय प्रक्रिया प्रभाव, विशेष रूप से चरम घटनाओं के लिए,मॉडल में पूर्वाग्रहों का प्राथमिक संपर्ककर्ता है। वर्तमान अध्ययन इस बात पर चर्चा करता है कि कैसे छोटे और बड़े पैमाने के सर्वोत्कृष्ट वातावरण में घटना की उत्पत्ति विभिन्न संवहन प्राचलीकरण के एक सेट के भीतर की जाती है। कुछ अंतर्निहित त्रुटियों के बावजूद,अधिकांश चयनित संवहन प्राचलीकरण योजनाएँ 10-15 दिन पहले उत्तराखंड में भारी वर्षा (2013) का संकेत दे सकती हैं,जो बड़े पैमाने पर पृष्ठभूमि की परस्पर क्रिया का परिणाम है। इस मामले में, बिना किसी संवहन योजना के चलने वाली रन्स,इसके बाद नई-टाइडटके और BMJ योजनाएं बेहतर प्रदर्शन करती हैं। इसके अलावा,नई-टाइडटके को छोड़कर लगभग सभी योजनाएँ माउंट-आबू बाढ़ (2017) के मामले में देखी गई विशेषताओं को पेश करने में विफल रहीं, जो कि 5-दिवसीय अग्रिम प्रारम्भण सहित सापेक्ष स्थानीय स्तर की परस्परक्रिया से उत्पन्न हुई थीं । दोनों चरम घटनाओं के सर्वश्रेष्ठ प्रदर्शनकर्ताओं का उपयोग करके और अधिक कुशल न्यू-टाइडटके के परिणामों को कुछ अन्य मामलों के लिए आगे बढ़ाया जाता है। इस योजना में संवहनी प्रेषण (विशेष रूप से उथले भाग के लिये) और कम बादलों का बेहतर निरूपण इसे अत्यधिक वर्षा की घटनाओं के अनुकरण के लिए अन्य योजनाओं से बेहतर बनाता है।

ABSTRACT. Approximated and simplified real-atmospheric process impact in physical parameterization is a primary correspondent of biases in the model, particularly for extreme events. The present study discusses how event genesis in the small and large-scale quintessential environment is simulated within a set of different convection parameterizations. Despite a few inherent errors, most of the selected convective parameterization schemes could indicate 10-15 days in advance the Uttarakhand heavy rains (2013) resulted from large-scale background interaction. The runs without any convection scheme, followed by new-Tiedtke and BMJ schemes, outperform in this case. Further, almost all schemes except new-Tiedtke failed to reproduce observed characteristics for the case of Mount-Abu flood (2017) originated from relatively local-scale interaction even from 5-day advance initialization. Results are further extended for a few other cases using best performers of both extreme events and new-Tiedtke found to be more efficient. The better representation of convection (especially the shallow) and low clouds in this scheme makes it superior to other schemes for simulating extreme precipitation events.

Key words – Extreme rainfall, Uttarakhand.

1. Introduction

The success of regional simulations is strongly associated with the boundary forcing used to drive the model and the physical parameterizations selected for the integration (Xue *et al*., 2014). Stensurd *et al*. (2000) elucidate that the model physics primarily determines the evolution of weather events in the absence of strong environmental forcing. However, the lateral boundary conditions (LBCs) decide the event development when the large-scale background signals are relatively strong. Hence, one would expect regional simulation to be influenced by the errors imbibed from poor LBCs and assumptions in model physical parameterizations (Xu and Yang, 2012).

Physical parameterization is at the heart of weather prediction because it influences temperature and rainfall, two necessary meteorological fields of forecasting interest. Convection, cloud formation and associated processes influence precipitation production and play a vital role in transporting moisture, momentum and heat in

atmospheric columns and significantly impact the large-scale dynamics (Arakawa and Schubert, 1974; Kain and Fritsch, 1990). The numerical weather prediction models have parameterized sub-grid scale convection categorized as deep and shallow convection. Deep convection involves intense vertical ascent, condensational latent heat release, higher cloud tops reaching tropopause and downpours (Zhang and Chou, 1999). Furthermore, the updrafts from surface to top of the planetary boundary layer are considered as shallow convection. Most convective schemes have a unified treatment of these convection types (Randall, 1989; Emanuel *et al*., 1994; Lopez, 2007). The microphysical processes in resolved clouds like the formation of water species, their growth and fallouts are accounted for by microphysics parameterization (Sundqvist, 1978). Model errors are primarily sourced from approximations of these parameterized processes in the microphysics and convection schemes (Stensrud *et al*., 2015).

Weather Research and Forecasting (WRF) model provides a wide range of physical parameterization schemes and earlier authors have compared WRF simulations for extreme events using these different schemes and shown the sensitivity of simulated case studies to the selected parameterizations (Rajeevan *et al*., 2010; Osuri *et al*., 2012; Alam, 2014; Diaz *et al*., 2015; Tahir *et al*., 2015; Yang *et al*., 2019; Hunt and Menon, 2020). However, the results vary significantly in each study and regardless of comprehensive studies, there is no consensus for any scheme to consistently perform well. It can be expected since the regional simulations are controlled by multiple factors such as study area, model domain, resolution, LBCs and domain nesting (Xue *et al*., 2014). Nonetheless, it is essential to untangle the probable biases introduced by different schemes to improve the understanding and applications of the regional model. Therefore, the present study investigates the feasibility of instigated errors in extreme event simulation using various convection schemes. Moreover, to avoid ambiguities between boundary conditions parented errors and model physics errors, the sensitivity to physics is trailed using ERA5 reanalysis data as LBCs.

The paper is systematized in four sections, including the current introduction section. Methodology and data-sets used for the study are described in section 2. The subsequent section 3 is dedicated to the results, followed by the summary of findings in section 4.

2. Data and methodology

WRF model (Skamarock *et al*., 2019) has been used for convection scheme sensitivity. The selected regional domain extends from 25° S-55° N, 30° E-128° E with horizontal spatial resolution of 9km and 37 vertical levels. Model set up work with Yonsei University (YSU) boundary layer scheme (Hong *et al*., 2006), Rapid-Radiative Transfer Model (Mlawer *et al*., 1997) longwave and Dudhia shortwave (Dudhia, 1989) radiation schemes and WRF single moment class-5 (WSM5) microphysics scheme (Hong *et al*., 2004).

The chosen cumulus schemes include Kain-Fritsch (KF) (John, 2004), Betts-Miller-Janjic (BMJ) (Janjić, 1994), Tiedtke (Tiedtke, 1989; Zhang, 2011), new Tiedtke (NTdke) (Zhang and Wang, 2017) and switching off the convection (noCU). The post-processing is done using Unified Post Processor (McKee *et al*., 2019). The meteorological variables mentioned in Table 1 from

TABLE 1

List of input variables given as ICs and LBCs to WRF-ARW

S. No.	Variable	Units
1.	Temperature	K
2.	U component of wind	m s^{-1}
3.	V component of wind	m s^{-1}
4.	Relative Humidity	%
5.	Height	m
6.	Sea-level Pressure	Pa
7.	Temperature at 2 m	K
8.	Relative Humidity at 2 m	%
9.	Specific Humidity	kg kg^{-1}
10.	U component of wind at 10 m	m s^{-1}
11.	V component of wind at 10 m	m s^{-1}
12.	Surface Pressure	Pa
13.	Soil Moist 0-10 cm below ground layer (Up)	Fraction
14.	Soil Moist 10-40 cm below ground layer	fraction
15.	Soil Moist 40-100 cm below ground layer	fraction
16.	Soil Moist 100-200 cm below ground layer	fraction
17.	T 0-10 cm below ground layer (Upper)	K
18.	T 10-40 cm below ground layer (Upper)	K
19.	T 40-100 cm below ground layer (Upper)	K
20.	T 100-200 cm below ground layer (Bottom)	K
21.	Ice flag	proportion
22.	Land/Sea flag (1=land, 0 or 2=sea)	proportion
23.	Terrain field of source analysis	m
24.	Skin temperature (can use for SST also)	K
25.	Water equivalent snow depth	kg m^{-2}

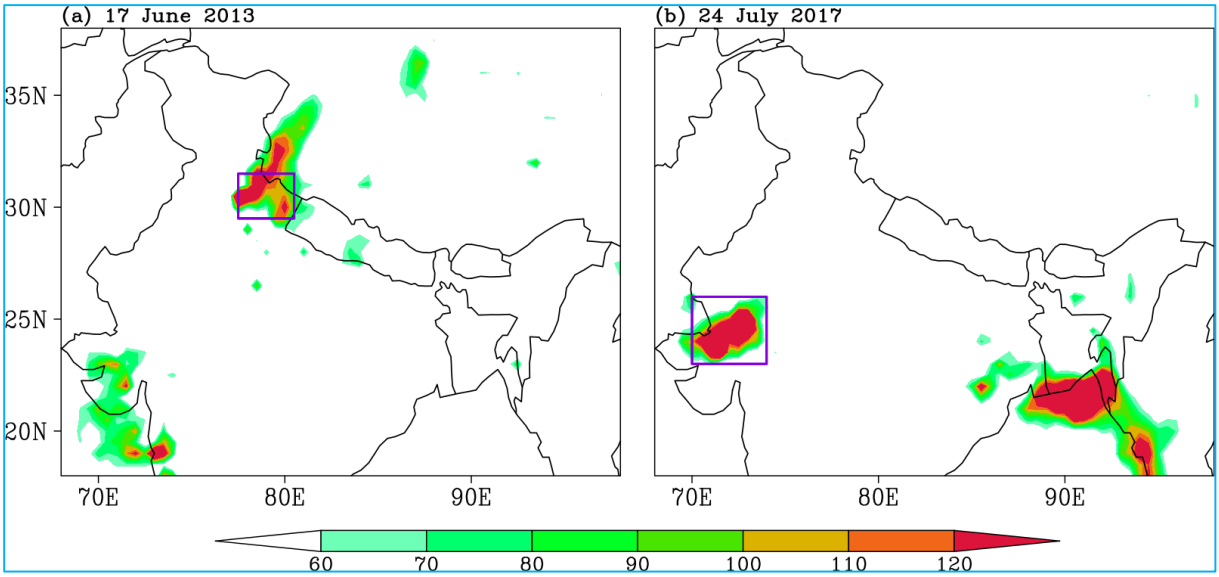

Figs. 1(a&b). Observed rainfall (mm/day) during (a) Uttarakhand event 17th June, 2013 and (b) Mount Abu event 24th July, 2017. The area selected for the event analysis is enclosed by purple rectangle in the figures

TABLE 2

Details of the physics run in terms of parameterization schemes used

S. No.	Run (Microphysics + Convective scheme)	Description
1.	noCU (WSM5 + convection off)	WRF single moment class 5 (WSM5) (Hong *et al*., 2004) microphysics scheme permits no super cooled water and the snow melts below the melting layer
2.	KF (WSM5 + Kain – Fritsch)	KF convective scheme (Kain, 2004) A mass flux scheme having moist updrafts and downdrafts, entraining and detraining cloud, hydrometeors rain, ice and snow. The closure used for deep convection is CAPE removal, whereas for shallow convection is based on TKE
3.	BMJ (WSM5 + Betts – Miller – Janjic)	BMJ convective scheme (Janjic´, 1994) An adjustment scheme that relaxes moisture and temperature profiles to reference profiles for both shallow and deep convection.
4.	Tiedtke (WSM5 + Tiedtke)	Tiedtke convection scheme (Tiedtke, 1989; Zhang *et al*., 2011) Amass-flux scheme with organized updrafts and downdrafts, turbulence entrainment and detrainment and CAPE based trigger and closure assumptions.
5.	NTdke (WSM5 + New – Tiedtke)	New-Tiedtke convection scheme (Zhang and Wang, 2017) Based on Tiedtke scheme but 1. It has a modified trigger and closure for deep and shallow. 2. The new entrainment and detrainment rates are introduced for different convection types, *i.e*., shallow, deep and mid-level convections. 3. It includes convective-induced pressure gradient linked to convective momentum transport. 4. It has a modified conversion formula for cloud water/ice to rain/snow

ERA5 reanalysis data (Hersbach *et al*., 2020) are given as LBCs to WRF. Table 2 describe the physics runs made to analyze event simulation based on the genesis background scenario.

The model output is compared against India Meteorological Department (IMD) rainfall observations (Mitra *et al*., 2009; Pai *et al*., 2014) for rainfall and ERA5 reanalysis for variables other than rainfall.

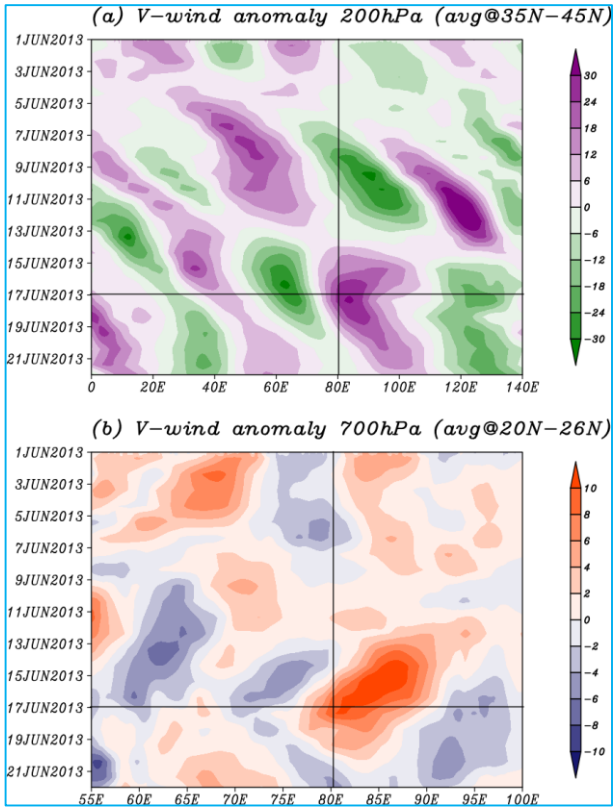

Figs. 2(a&b). Meridional wind (m/s) anomaly during Uttarakhand heavy rains (2013) at (a) 200 hPa representing the propagation of trough in upper level westerlies and (b) 700 hPa for advancement of low-pressure system from head Bay. The vertical (horizontal) black line represents the longitude (date) of the event

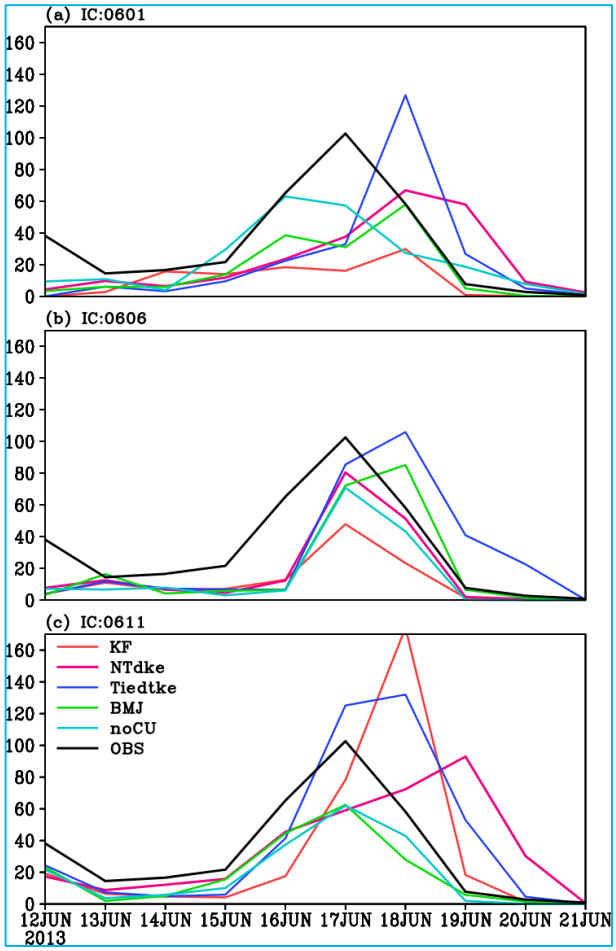

Figs. 3(a-c). Time-series of area-averaged rainfall (mm/day) during Uttarakhand event (17th June, 2013) from observation (black) and physics simulations (multi-color) from (a) farthest IC (0601), (b) far IC (0606) and (c) near IC (0611)

3. Results and discussion

3.1. *Event background and simulation*

The results from the physics run (Table 2) for two events having different genesis conditions are discussed in subsequent subsections. These events include (*i*) Uttarakhand heavy rainfall 2013 and (*ii*) Mount Abu Flood 2017, in subsections 3.1.1 and 3.1.2, respectively. Figs. 1(a&b) show observed rainfall for these two events with a rectangular box representing the area selected for event analysis.

3.1.1. *Uttarakhand heavy rainfall*

On 17 June, 2013, the heavy downpours lashed out over more than 4000 villages of northern Indian state Uttarakhand (Houze *et al*., 2017). The event was reported as one of the worst meteorological occurrences with severe loss of lives and property. Many studies attempted to unveil the mechanisms behind the event (Dube *et al*., 2014; Singh *et al*., 2014; Joseph *et al*., 2015; Nandargi *et al*., 2016; Houze *et al*., 2017; Kedia *et al*., 2019) which was known to result from large-scale interaction between a trough in the mid-latitude upper-level westerlies and west-northwestward moving low-pressure systems from Bay of Bengal (BoB). Fig. 2(a) shows the Rossby wave train in 200 hPa meridional wind anomaly reaching the Uttarakhand region on the event day. Simultaneously, the BoB low-pressure system shown by the 700 hPa meridional wind anomaly in Fig. 2(b) approached the region. Joseph *et al.* (2015) elaborated on the large-scale interactions between these two weather systems.

The different physics options selected for the study could indicate the event 15 days advance [Fig. 3(a)], although the rainfall maximum is misrepresented in all physics. At ten days lead [Fig. 3(b)], the signal for eminent precipitation is much more precise than 15 days

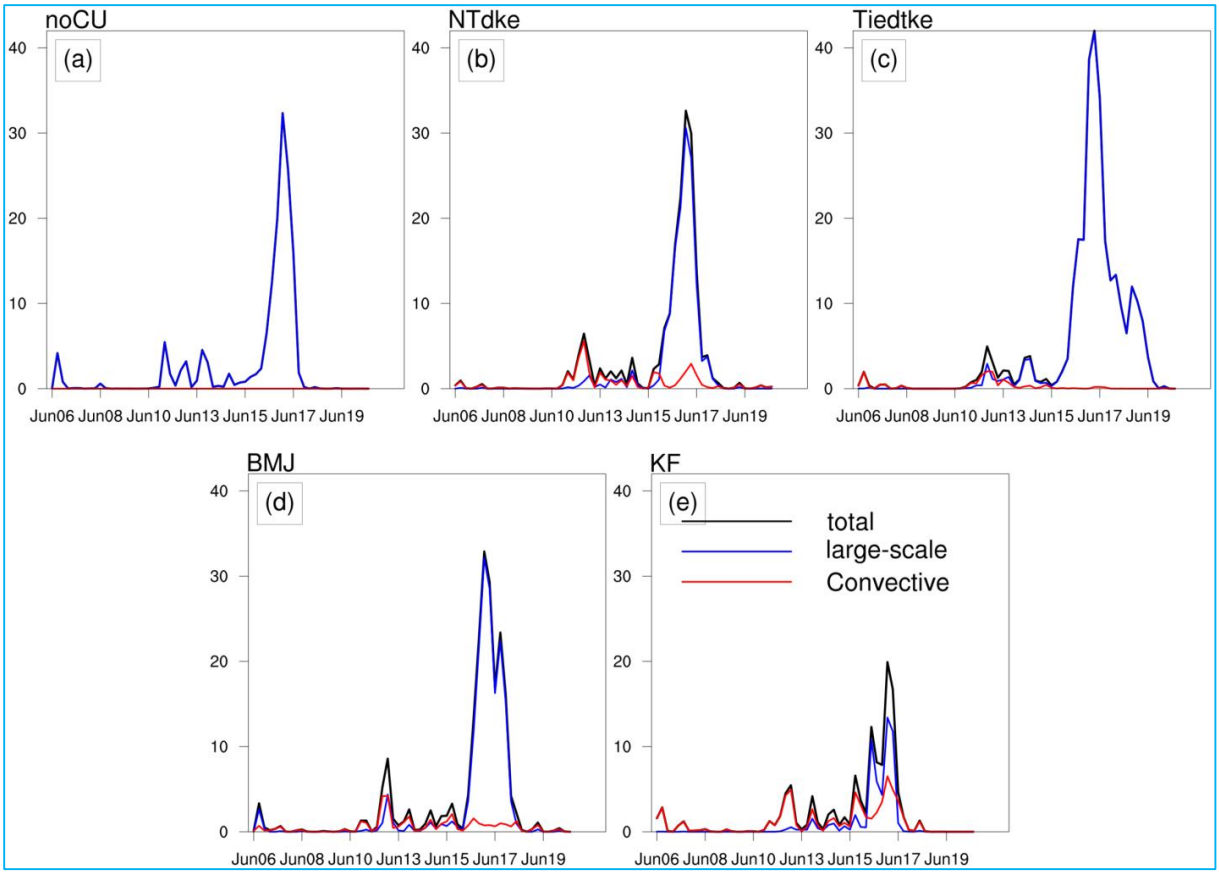

Figs. 4(a-e). Temporal distribution of total (black), large-scale (blue) and convective (red) rainfall (mm/6 hour) during Uttarakhand event (17th June, 2013) from (a) noCU, (b) NTdke, (c) Tiedtke, (d) BMJ and (e) KF physics run of IC 0606

lead in all physics. From the nearest initialization, *i.e.*, five days ahead [Fig. 3(c)], most physics runs deviate from the observation. The simulation without convection scheme consistently reproduced rainfall peak on 17 June despite an underestimated amplitude at all three leads.

The run with KF convection largely under-predicted the precipitation for both 15 and 10 days lead time, whereas it overestimated the rainfall at five days lead with a one-day temporal shift. KF scheme activates convection depending upon the grid-resolved ascents (Kain, 2004). Therefore, it is speculated that the strong vertical velocity in an event near initialization, *i.e.*, 0611 has more active convection and hence raining exceptionally high, whereas the convection is comparatively dampened in KF runs initialized from 0606 and 0601 ICs. Tiedtke run shows overestimation and temporal shift in rainfall maximum at all the three leads. BMJ could not perform well with a 15-day lead, but simulation improved ten days advance and at five days lead, it shows temporal accuracy although with lesser-than-observed magnitude in rainfall. The NTdke run is more reasonable at a ten-day lead than all other physics in terms of temporal position and intensity of rainfall maximum, but it shows a delayed peak in the runs that are initialized 15 and 5 days before the event.

Convective and large-scale rainfall plot [Figs. 4(a-e)] from 10 days advance run (*i.e.*, simulation with more accuracy in general for all) is consistent with the temporal distribution [Figs. 3(a-c)] discussed above. All physics options show more rainfall contribution from large-scale than the convective. Tiedtke overestimates the large scale rainfall, whereas KF underestimates it. BMJ simulated large-scale rainfall peak is a little broader and has two spikes. NTdke and noCU runs have comparable large-scale rainfall, but NTdke has an additional contribution from convective scale; hence the total rainfall is slightly closer to observed rainfall than noCU.

3.1.2. *Mount Abu flood*

The northwestern region of India received torrential rains on 24th July, 2017, which spawned severe flooding, deaths and property damage (Peatier, 2017; Ray *et al.*,

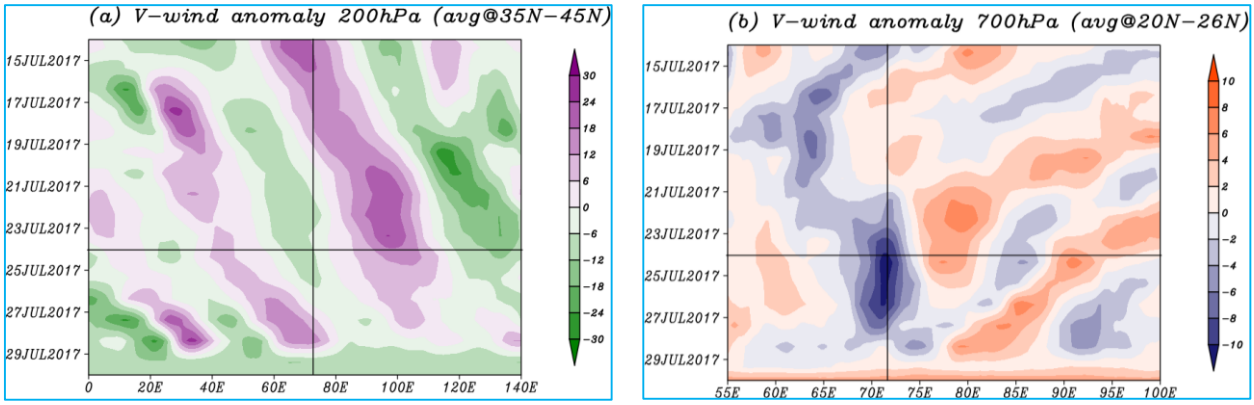

Figs. 5(a&b). Same as Fig. 2, but for the Mount Abu flood (24 July, 2017)

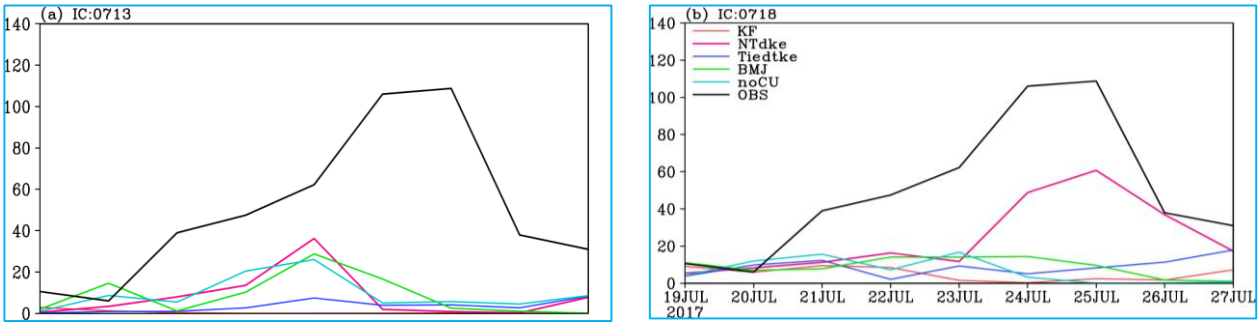

Figs. 6(a&b). Time-series of area-averaged rainfall (mm/day) during Mount Abu flood (24 July, 2017) from observation (black) and physics simulations (multi-colour; kindly refer legend) from (a) far IC (0713) and (b) near IC (0718)

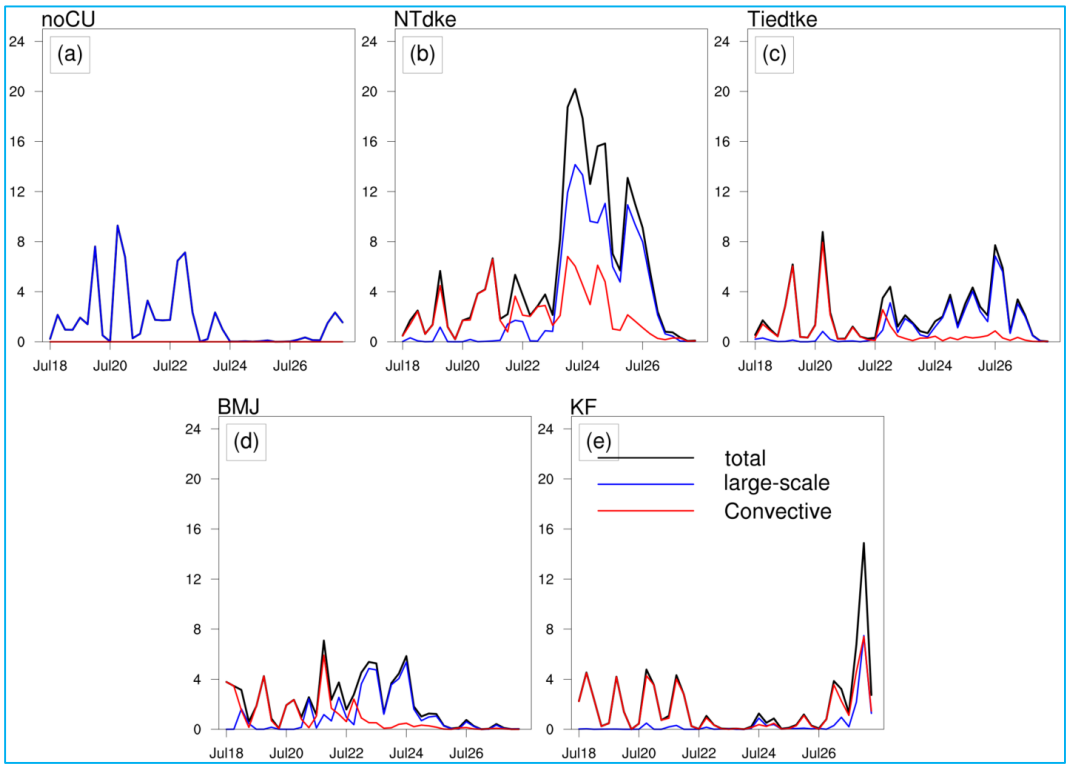

Figs. 7(a-e). Temporal distribution of total (black), large-scale (blue) and convective (red) rainfall during Mount Abu flood (24th July, 2017) from (a) noCU, (b) NTdke, (c) Tiedtke, (d) BMJ and (e) KF physics runs of IC 0718

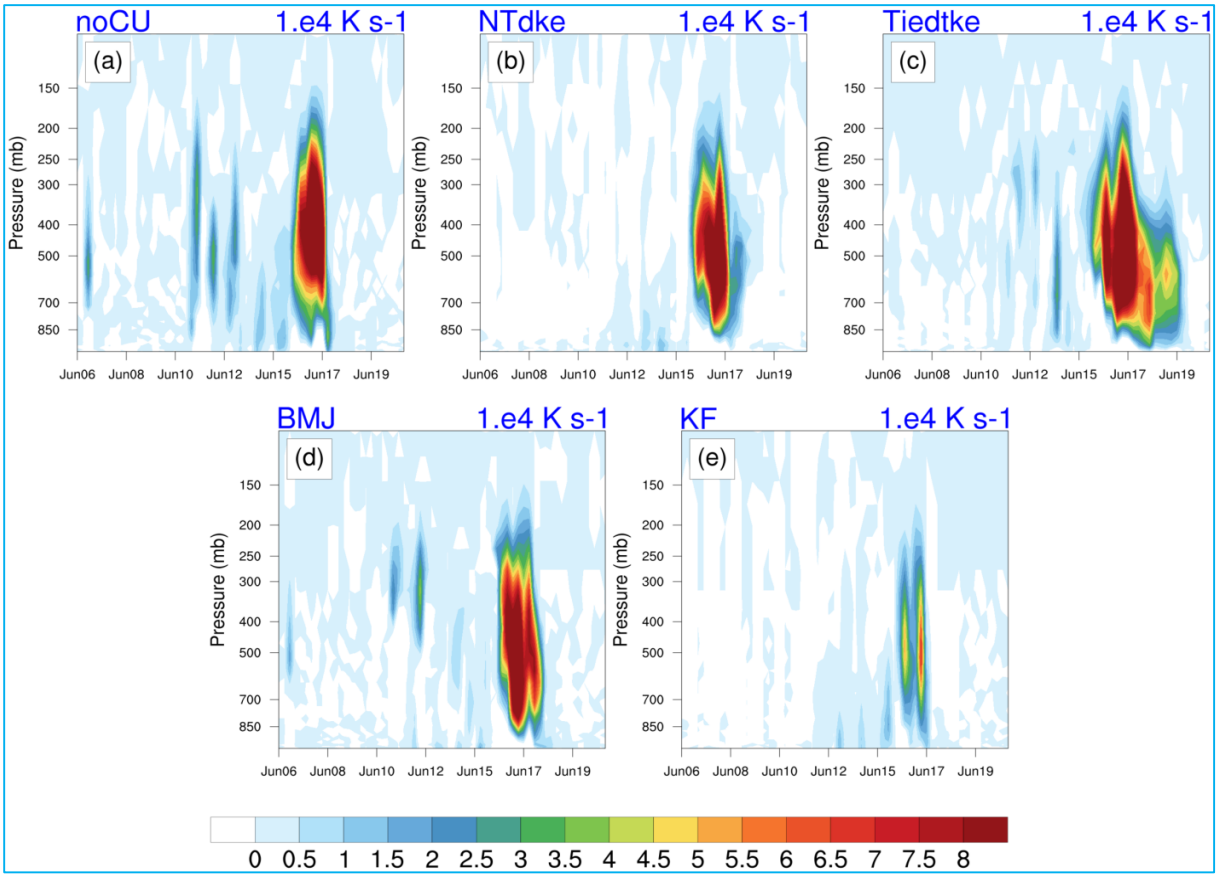

Figs. 8(a-e). Temporal evolution of atmospheric profile of microphysical diabatic heating (K s−1) tendencies over the Uttarakhand event region (17th June, 2013) from (a) noCU, (b) NTdke, (c) Tiedtke, (d) BMJ and (e) KF physics run of IC 0606

2019). The event genesis occurred in a pre-conditioned atmosphere from back-to-back northwestward moving disturbances from BoB and local-circulation hovering over the region. Fig. 5(a) shows the absence of well-defined Rossby wave trains in the upper level, whereas a less intense and dissipating system from BoB over the region can be seen in Fig. 5(b). Overall the system was originated from relatively local scale conditions in contrast to the Uttarakhand event.

The model physics simulations could not capture this event 15 days in advance (figure not shown). Most of the schemes have difficulty simulating the event 10 days or even 5 days in advance [Figs. 6(a&b)]. Out of all the selected parameterizations, only NTdke scheme (magenta colour line) could give some indication of the event at 10 days lead, but underestimated and temporally shifted the rainfall peak. Both the intensity of the rainfall and temporal shift in NTdke run has improved in 5-day advance simulation.

Convective and large-scale rainfall temporal distribution from 5-day lead [Figs. 7(a-e)] also show that peaks in both rain types are absent on 24 July in most of the physics runs. It is only NTdke which has both large-scale as well as convective rainfall adding up to give a rainfall maximum on 24 July.

3.2. *Model physics tendencies and cloud-fraction*

Looking at the physics tendencies, microphysical heating dominates during the Uttarakhand event in all physics runs with a 10-day lead [Figs. 8(a-e)]. Tiedtke and BMJ temporally extend the microphysical heating maximum similar to the rainfall, with the Tiedtke scheme overestimating the magnitude as well. However, KF is underestimating it to quite an extent. Convection switched-off (noCU) run and NTdke exhibit somewhat alike heating. The convection heating contributes quite less during the event [Figs. 9(a-d)]. Tiedtke and BMJ runs have even smaller convective heating. KF has a little stronger convective heating tendency but since its large-scale counterpart is not fairly captured, it ends up underestimating the overall heating and hence precipitation during the event. NTdke has higher convective heating complimenting well the microphysics.

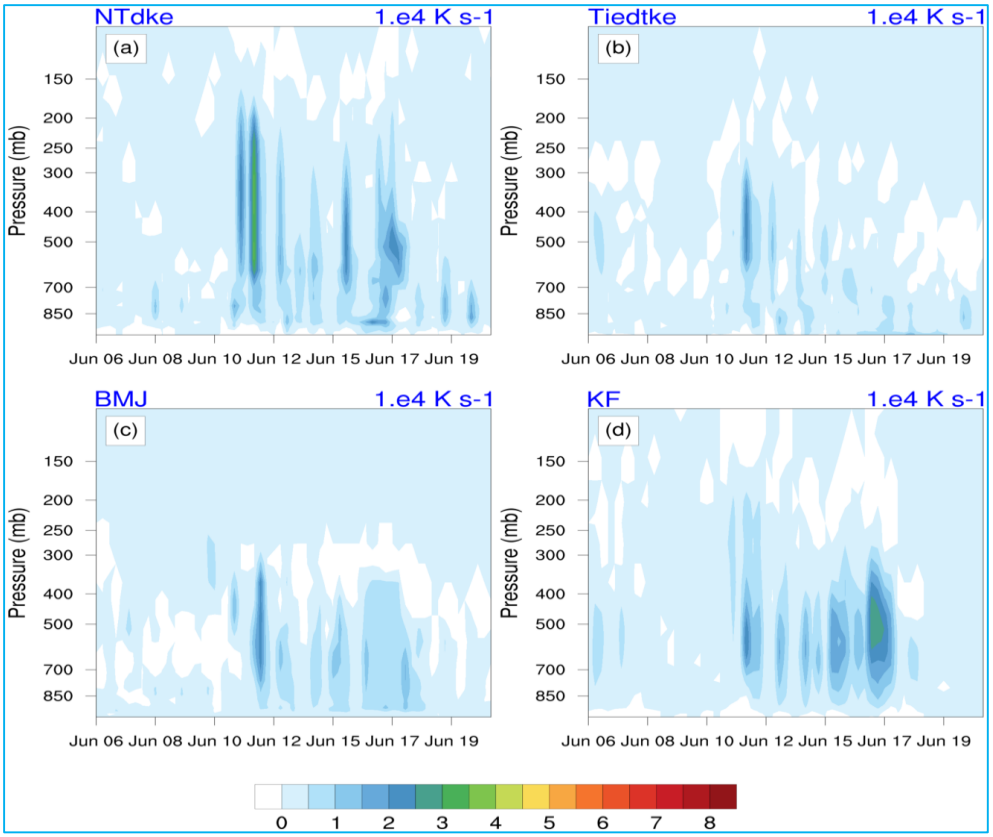

Figs. 9(a-d). Temporal evolution of atmospheric profile of convective diabatic heating (K s^{-1}) tendencies over Uttarakhand event region from (a) NTdke, (b) Tiedtke, (c) BMJ and (d) KF physics run of IC 0606

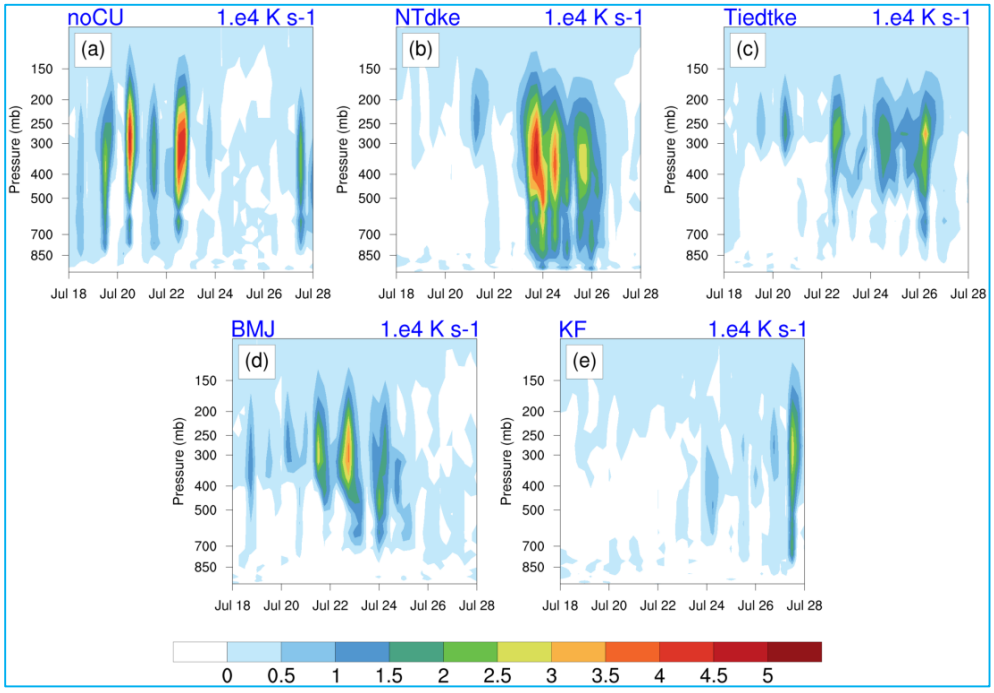

Figs. 10(a-e). Temporal evolution of atmospheric profile of microphysical diabatic heating (K s^{-1}) tendencies over Mount Abu flood region (24th July, 2017) from (a) noCU, (b) NTdke, (c) Tiedtke, (d) BMJ and (e) KF physics run of IC 0718

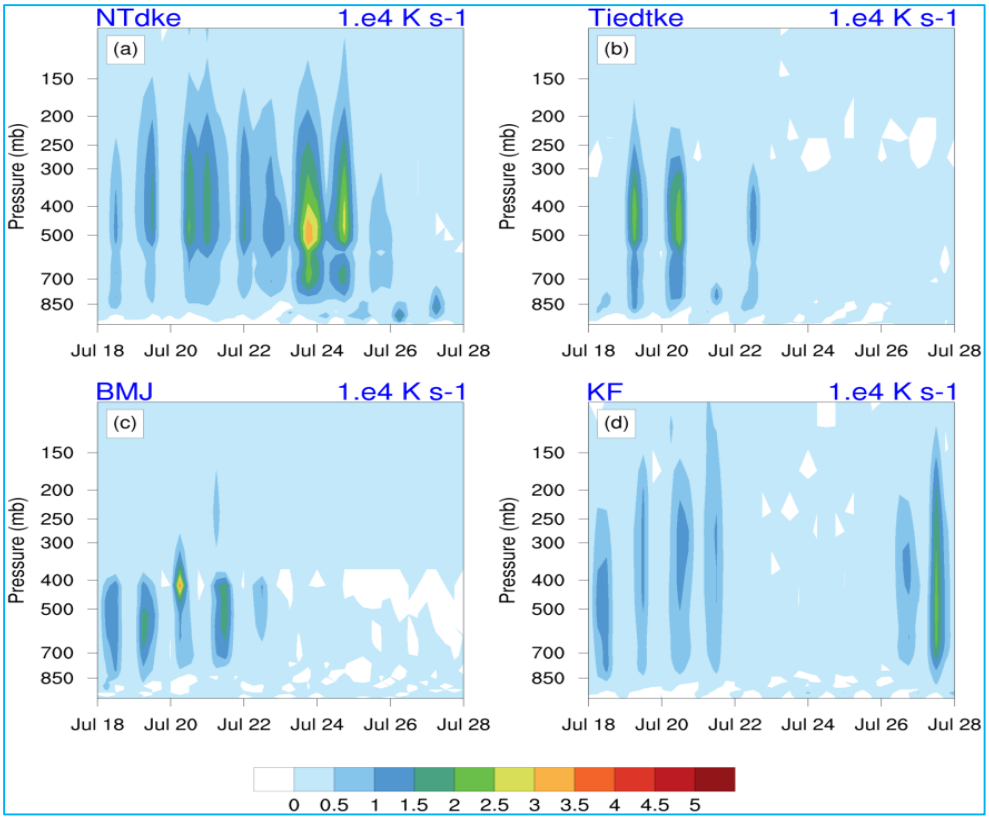

Figs. 11(a-d). Temporale volution of atmospheric profile of convective diabatic heating (K s^{-1}) tendencies over Mount Abu flood region (24th July, 2017) from (a) NTdke, (b) Tiedtke, (c) BMJ and (d) KF physics run of IC 0718

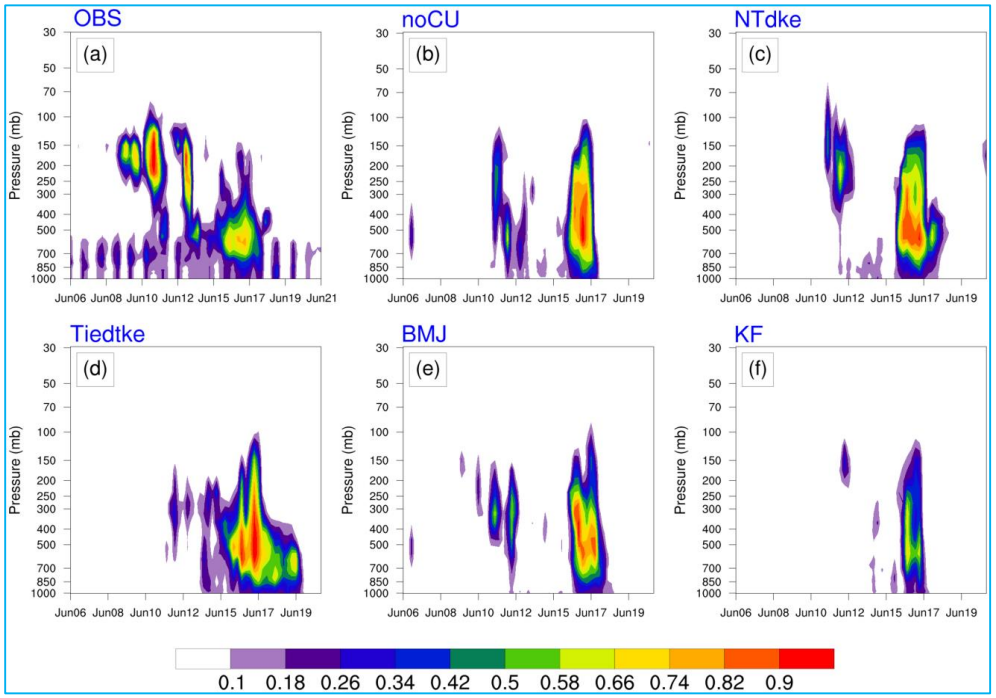

Figs. 12(a-f). Time-height distribution of cloud-fraction from (a) ERA5 reanalysis, (b) noCU, (c) NTdke, (d) Tiedtke, (e) BMJ and (f) KF physics runs over the region of Uttarakhand heavy rainfall event (17th June, 2013)

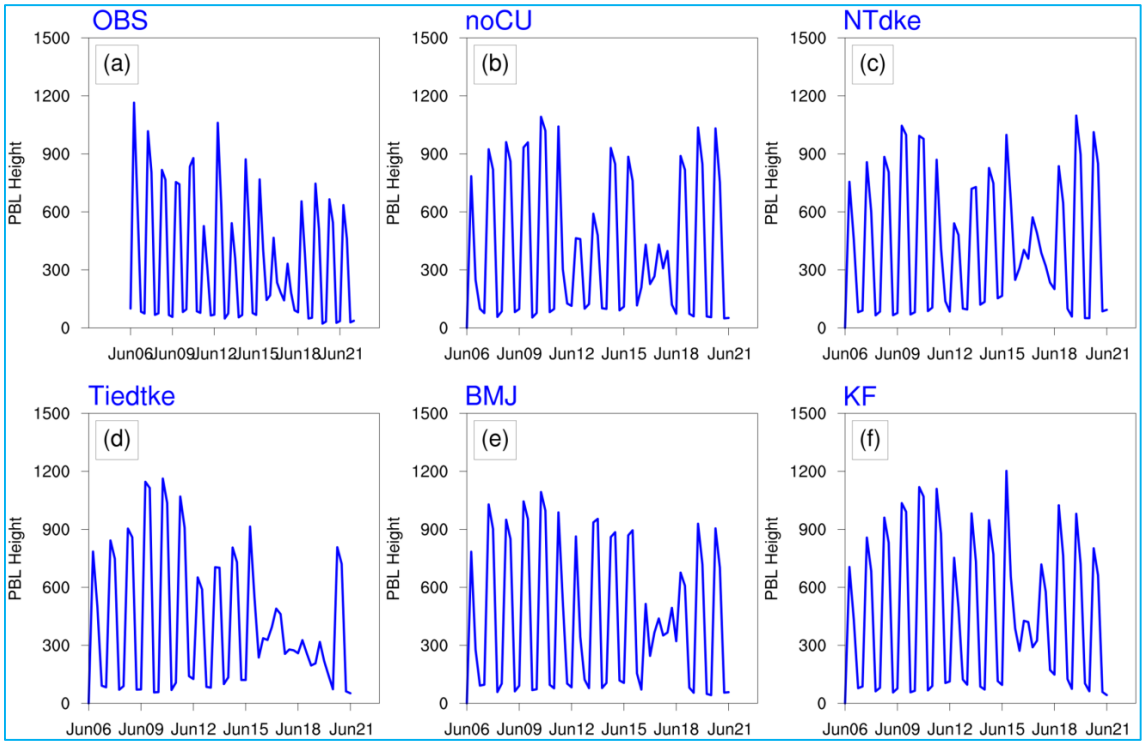

Figs. 13(a-f). Temporal distribution of boundary layer height from (a) ERA5 reanalysis, (b) noCU, (c) NTdke, (d) Tiedtke, (e) BMJ and (f) KF physics runs during Uttarakhand heavy rains (17th June, 2013)

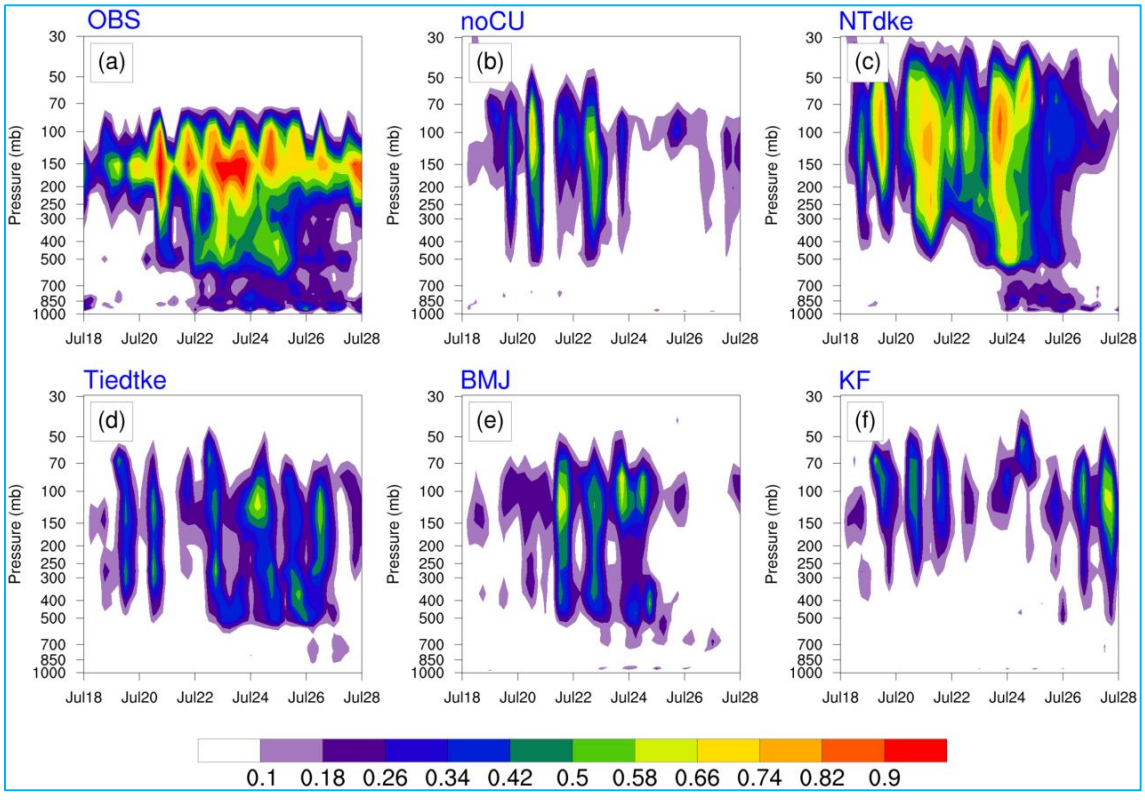

Figs. 14(a-f). Time-height distribution of cloud-fraction from (a) ERA5 reanalysis , (b) noCU, (c) NTdke, (d) Tiedtke, (e) BMJ and (f) KF physics runs over Mount Abu flood region (24th July, 2017)

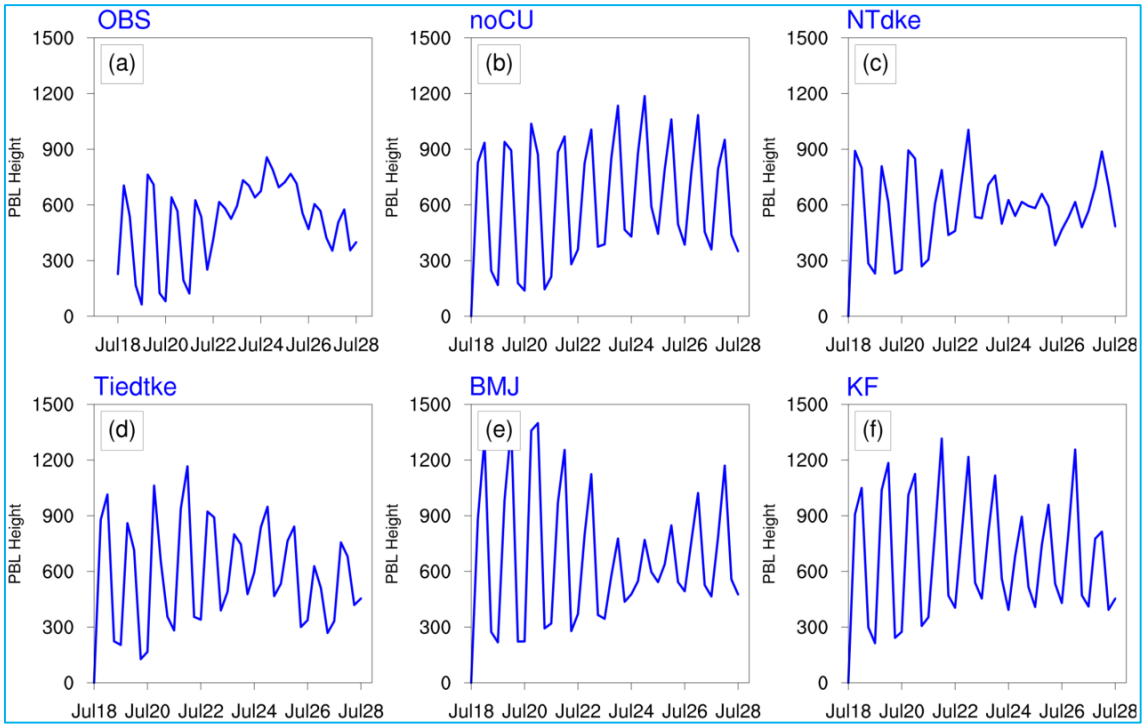

Figs. 15(a-f). Temporal distribution of boundary layer height from (a) ERA5 reanalysis, (b) noCU, (c) NTdke, (d) Tiedtke, (e) BMJ and (f) KF physics runs during Mount Abu flood (24th July, 2017)

Moisture tendencies also reflect similar results; Tiedtke and BMJ have more large-scale moisture compared to convective scale (figure not shown). NTdke tries to capture the moisture temporal profile comparable to the noCU.

Contrary to the Uttarakhand case, the large-scale [Figs. 10(a-e)] and convective [Figs. 11(a-d)] heating tendencies have less difference during Mount Abu Flood. Most of the physics runs showed the inability to reproduce heating maximum on 24 July, especially for convective scale. Tiedtke and BMJ have incapacitated microphysical heating tendencies at upper levels and even poorer convective scale heating. NTdke tendencies match fairly well with the rainfall peaks, the enhanced moisture and heating can be found in the atmospheric profile simulated by NTdke on the event day in both types of tendencies. NTdke convective moisture tendencies are stronger in the lower troposphere, whereas convective heating is more around 500 hPa but still lower than the microphysical heating maximum.

The above described tendencies explain quite a lot about both events, summing it up in the cloud distribution plotted in Figs. 12(a-f) and Figs. 14(a-f) for ERA5 reanalysis and physics runs. The cloud maximum concerning the Uttarakhand event [Figs. 12(a-f)] is captured fairly well by the model regardless of the chosen convective parameterization or even after turning off the convection. The large-scale associated signal present in LBCs made the event more predictable. Closely observing the figure, the individual schemes have variations in reproducing cloud distribution, for example, Tiedtke extends and overestimate the total cloud cover whereas KF cloud maximum is temporally shrunk and weaker than ERA5. Altogether, NTdke and noCU show superiority in capturing the overall distribution. A dip in boundary layer height from ERA5 reanalysis [Figs. 13(a-f)] around 17 June indicates the presence of clouds above the boundary layer. All physics simulations could reproduce the observed boundary layer height variations to a large extent [Figs. 13(b-f)].

The Mount Abu flood was a relatively smaller-scale and less predictable event as discussed in subsection 3.1.2. The ERA5 cloud distribution for event duration [Fig. 14(a)] depicts the presence of low-level clouds over the regions in addition to deep clouds at upper levels. Most of the physics runs [Figs. 14(b-f)] show underestimated cloud fraction only above 500 hPa with a total absence of low-level clouds. It is only the NTdke run where the model could capture the lower as well as upper-level cloud fraction to a reasonable extent. The ERA5 reanalysis shows an increase in boundary layer height during the Mount Abu event reassuring the occurrence of boundary layer clouds or low-level clouds [Fig. 15(a)].

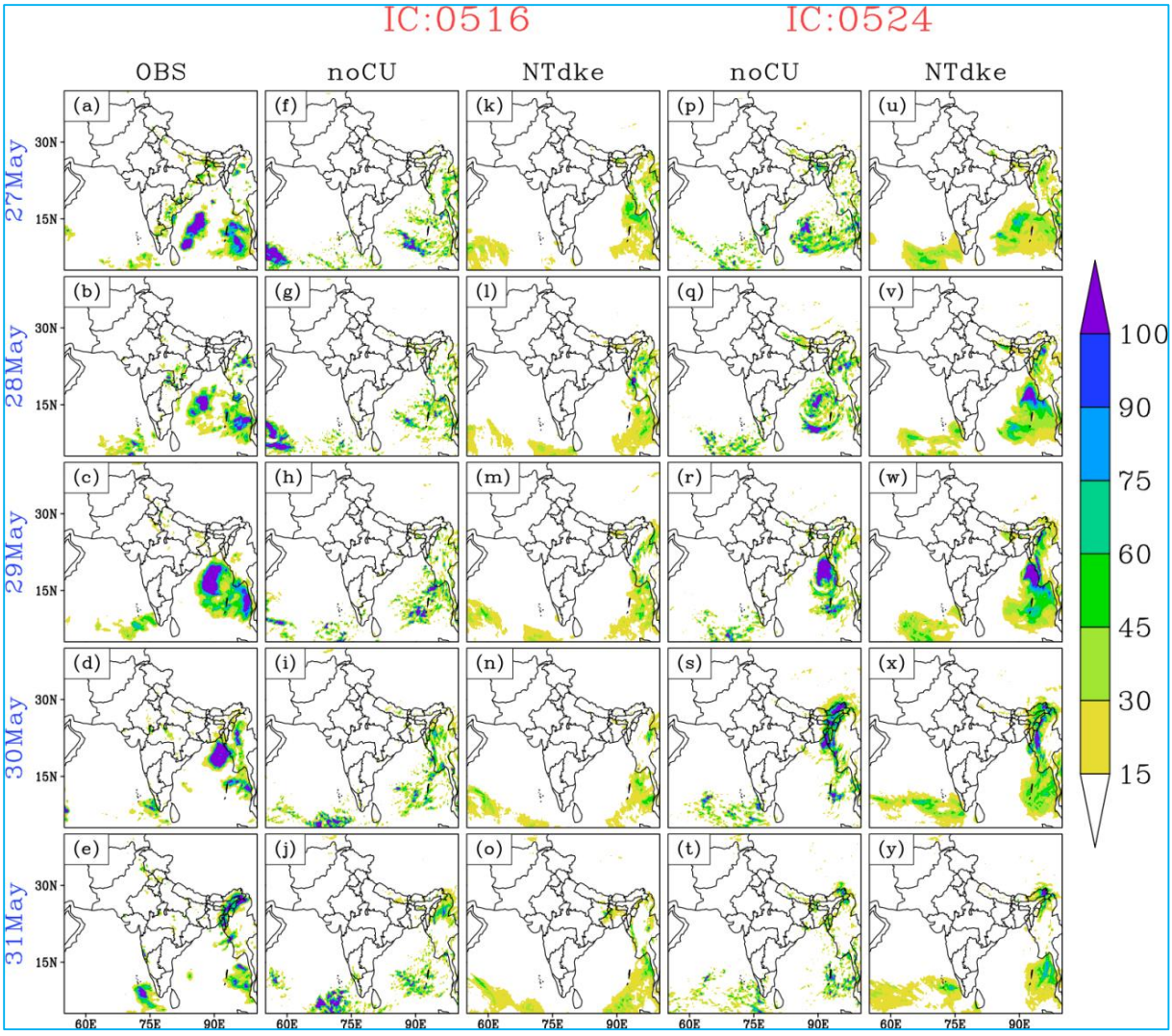

Figs. 16(a-y). Rainfall (mm/day) distribution for Mora cyclone during 27-31 May, 2017 (top-bottom) for (a-e) observation, (f-o) far IC (0516) and (p-y) near IC (0524) for noCU (f-j & p-t) and NTdke (k-o & u-y) physics runs

Furthermore, unlike Uttarakhand heavy rainfall case, the simulated height of the boundary layer [Figs. 15(b-f)] in the majority of physics runs does not alter the diurnal cycle of the BL height during the Mount Abu flood. Despite errors before and after the event, NTdke could capture the boundary layer height accurately around 24 July.

(Zhang, 2011) explain that KF and BMJ have difficulty in producing low-level or boundary layer clouds due to less active shallow parameterization in these schemes, which could lead to poor interaction with other physics components of the model during integration. The NTdke is a revamped version of Tiedtke in almost all aspects (Table 2), most importantly the NTdke is designed to better represent shallow, mid, as well as deep convection. Therefore, NTdke has a better representation of low-level to deep clouds for both events.

3.3. *Performance comparison of no-Convection and new-Tiedtke runs*

In the previous subsections, performance analysis of different physics highlights the better performanceof NTdke in two different event scenarios. To test whether or not these inferences stand true; the analysis has been extended to a few other cases selecting best performing physics runs for the two events, *i.e.*, noCU and NTdke. The selected cases are from the year 2017 and include the Mora cyclone, Mumbai heavy rainfall event and Ockhi cyclone.

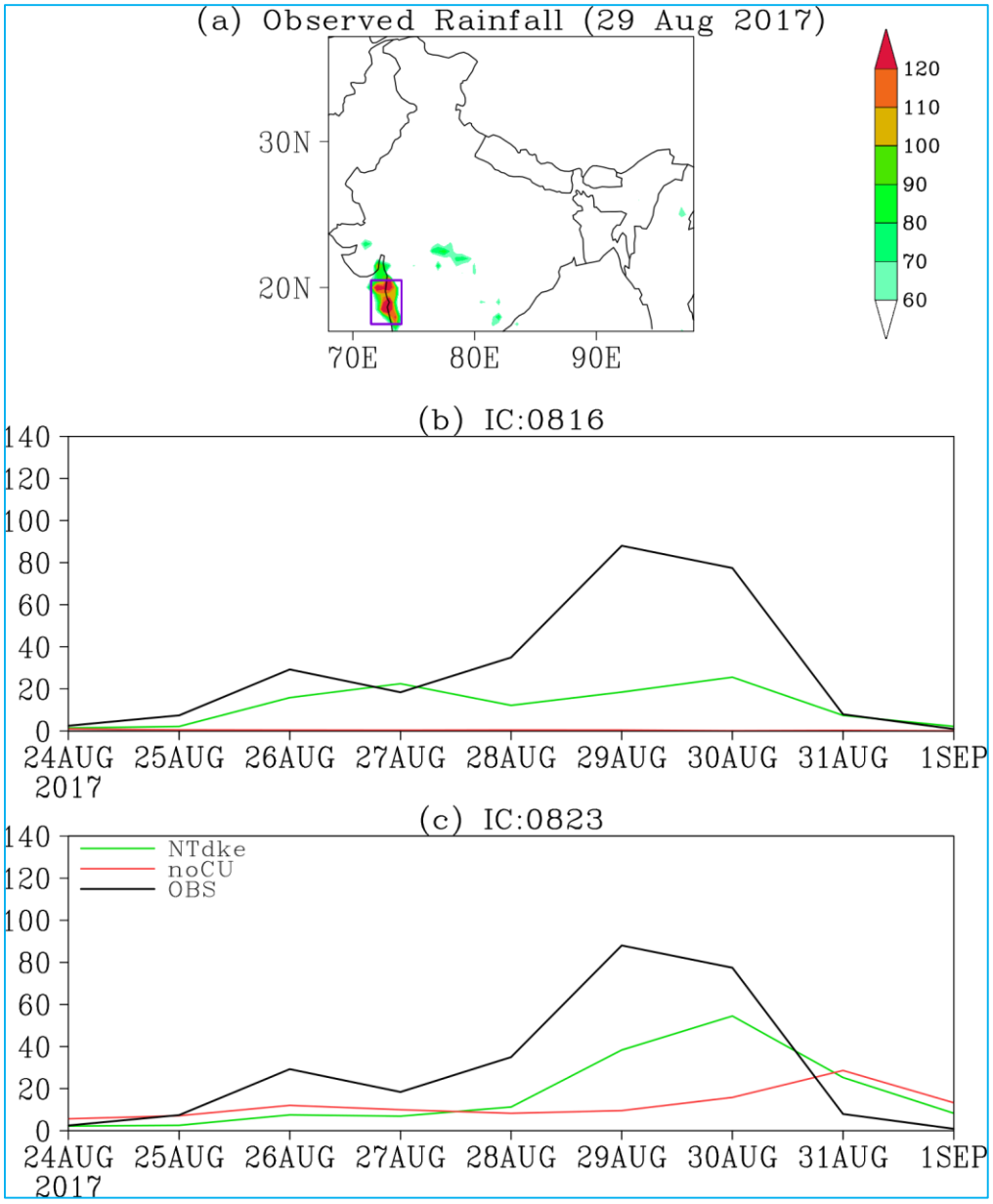

Figs. 17(a-c). (a) Spatial pattern of observed rainfall (mm/day) on 29 August, 2017 and area-averaged rainfall time-series from observation (black) and physics simulations (multi-color) from (b) far IC (0816) and (c) near IC(0823) for Mumbai heavy rainfall event

Figs. 16(a-y) show the genesis and progression of Mora cyclone from a near (0524) and far (0516) IC, both noCU [Figs. 16(f-j)] and NTdke [Figs. 16(k-o)] could not predict the system from far IC. However, both runs from near initialization [Figs. 16(p-t & u-y)] captured the system nearly close to the observation. The Mumbai heavy rains, which was of relatively local scale precipitation, was poorly simulated by noCU run from both near (0823) and far IC (0816) [Figs. 17(a-c)]. NTdke could better predict the rainfall peak from near IC [Fig. 17(c)].

Ockhi cyclone associated rainfall distribution is plotted in Figs. 18(a-y) from observation and 22 November (1122) and 29 November IC (1129) simulations of noCU and NTdke. noCU run could predict system only from near IC [Figs. 18(p-t)] and system dissipated quickly before making landfall, noCU overestimated (underestimated) the evolution of a simultaneous system in BOB from far (near) IC as seen in Figs. 18(f-j) [Figs. 14(p-t)]. NTdke run from both ICs [Figs. 18(k-o) & (u-y)] performs much better compared to noCU in

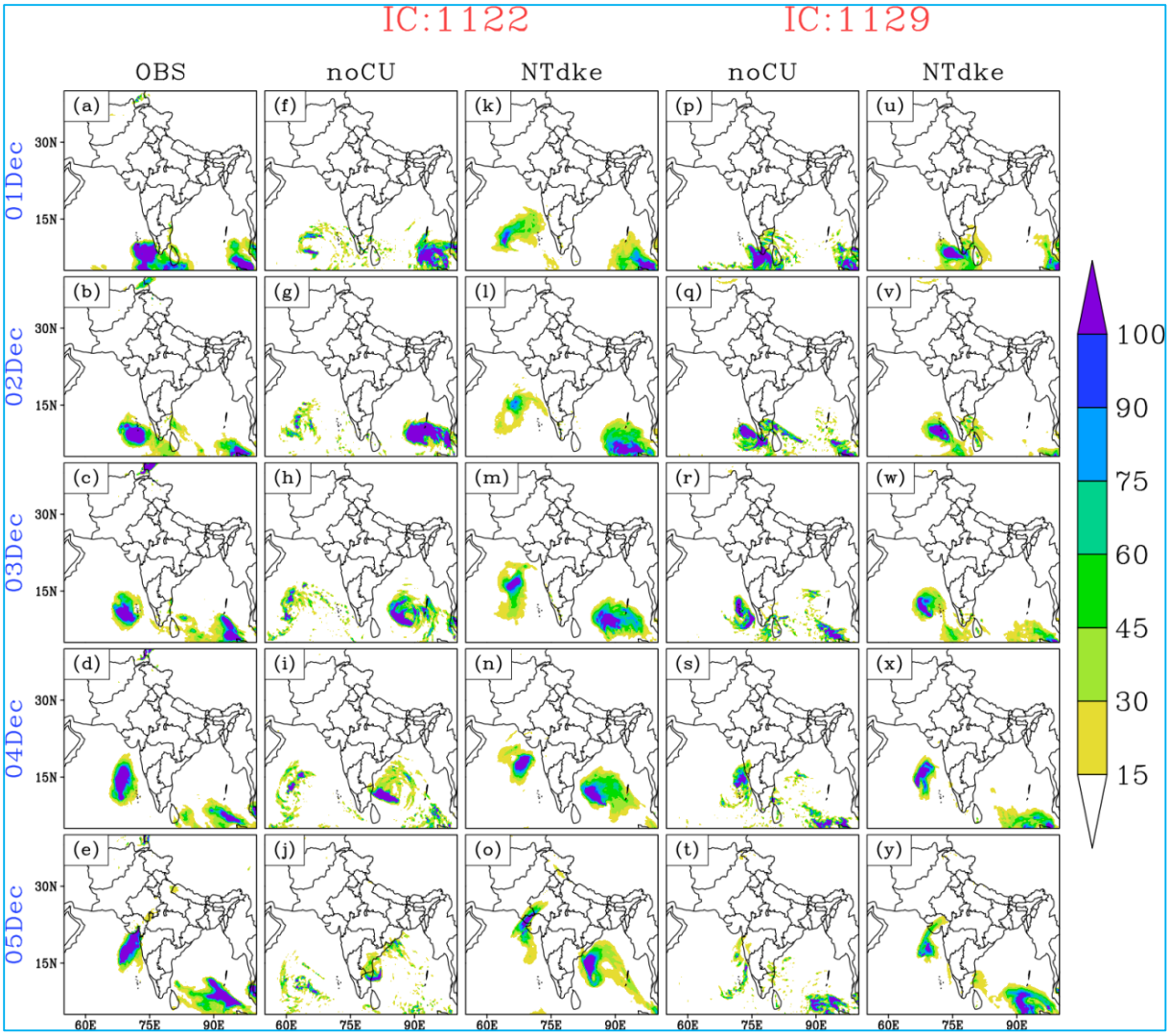

Figs. 18(a-y). Rainfall (mm day^{-1}) distribution for Ockhi cyclone during 01-05 Dec 2017 (top-bottom) for (a-e) observation, (f-o) far IC (1122) and (p-y) near IC (1129) for noCU (f-j & p-t) and NTdke (k-o & u-y) physics run

predicting the Ockhi cyclone. Especially the eastward recurvature under the influence of large-scale upper-level trough was captured exceptionally well by NTdke.

Therefore, it is incontrovertible that NTdke could better capture the extreme events connected with either small-scale or large-scale interactions of weather systems.

4. Conclusions

The convective trigger and closure assumptions and their interactions with other parameterized processes especially the resolved scale tendencies are likely to cause erroneous simulation (Kain and Fritsch, 1992; Suhas and Zhang, 2014). The chance of simulated fields deviating from observation increases in the absence of strong large-scale forcing. Therefore, the present study attempted to understand the biases due to convective parameterization in a regional modelling set-up for simulation of extreme precipitation under different scenarios of background interaction.

It has been shown that an event originating from large-scale interaction is well simulated by the majority of the selected convective parameterizations. Apart from the fact that different physics options have their limitations, the near-perfect boundary forcing alone enhance the likelihood of accurate prediction. Nonetheless, the physical schemes were unable to reproduce observed features in cases where local or sub-grid convection has an active role in determining the extreme precipitation.

However, the new-Tiedtke convective scheme stands out in reproducing the temporal and spatial location of extreme events originating in different convection scenarios, which could be attributed to its ability to accurately simulate different types of clouds in the atmospheric column.

Acknowledgements

Research at Indian Institute of Tropical Meteorology (IITM) is fully funded by the Ministry of Earth Science, Govt. of India. This work is part of Manpreet Kaur's Ph.D. thesis. The model runs and analysis is performed on Pratyush high performance computing facility at IITM.

Disclaimer : The contents and views expressed in this study are the views of the authors and do not necessarily reflect the views of the organizations they belong to.

References

Alam, M., 2014, "Impact of cloud microphysics and cumulus parameterization on simulation of heavy rainfall event during 7-9 October 2007 over Bangladesh", *J. Earth Syst. Sci*., **123**, 259-279. doi: 10.1007/s12040-013-0401-0.

Arakawa, A. and Schubert, W. H., 1974, "Interaction of a Cumulus Cloud Ensemble with the Large-Scale Environment, Part I", *J. Atmos. Sci*., **31**, 674-701. doi : 10.1175/1520-0469(1974)031<0674:IOACCE>2.0.CO;2.

Diaz, J. P., González, A., Expósito, F. J., Pérez, J. C., Fernández, J., García-Díez, M. and Taima, D., 2015, "WRF multi-physics simulation of clouds in the African region", *Q. J. R. Meteorol. Soc*., **141**, 2737-2749. doi : 10.1002/qj.2560.

Dube, A., Ashrit, R., Ashish, A., Sharma, Kuldeep, Iyengar, G. R., Rajagopal, E. N., Basu, Swati, 2014, "Forecasting the heavy rainfall during Himalayan flooding-June 2013", *Weather Clim. Extrem.*, **4**, 22-34. doi : https://doi.org/10.1016/j.wace.2014.03.004.

Dudhia, J., 1989, "Numerical study of convection observed during the Winter Monsoon Experiment using a mesoscale two-dimensional model", *J. Atmos. Sci*., **46**, 3077-3107.

Emanuel, K. A., David Neelin, J. and Bretherton, C. S., 1994, "On large-scale circulations in convecting atmospheres", *Q. J. R. Meteorol. Soc*., **120**, 1111-1143.

Hersbach, Hans, Bill Bell, Paul Berrisford, Shoji Hirahara, András Horányi, Joaquín Muñoz-Sabater, Julien Nicolas, Carole Peubey, Raluca Radu, Dinand Schepers, Adrian Simmons, Cornel Soci, Saleh Abdalla, Xavier Abellan, Gianpaolo Balsamo, Peter Bechtold, Gionata Biavati, Jean Bidlot, Massimo Bonavita, Giovanna De Chiara, Per Dahlgren, Dick Dee, Michail Diamantakis, Rossana Dragani, Johannes Flemming, Richard Forbes, Manuel Fuentes, Alan Geer, Leo Haimberger, Sean Healy, Robin J. Hogan, Elías Hólm, Marta Janisková, Sarah Keeley, Patrick Laloyaux, Philippe Lopez, Cristina Lupu, Gabor Radnoti, Patricia de Rosnay, Iryna Rozum, Freja Vamborg, Sebastien Villaume and Jean-Noël Thépaut, 2020, "The ERA5 global reanalysis", *Q. J. R. Meteorol. Soc*., **146**, 1999-2049. doi : 10.1002/qj.3803.

Hong, S., Dudhia, J. and Chen, S., 2004, "A Revised Approach to Ice Microphysical Processes for the Bulk Parameterization of Clouds and Precipitation", *Mon. Wea. Rev*., **132**, 103-120.

Hong, S., Noh, Y. and Dudhia, J., 2006, "A New Vertical Diffusion Package with an Explicit Treatment of Entrainment Processes", *Mon. Wea. Rev*., **134**, 2318-2341. doi : 10.1175/MWR3199.1.

Houze Jr., R. A., McMurdie, L. A., Rasmussen, K. L., Kumar, A. and Chaplin, M. M., 2017, "Multiscale Aspects of the Storm Producing the June 2013 Flooding in Uttarakhand, India", *Mon. Wea. Rev*., **145**, 4447-4466. doi : 10.1175/mwr-d-17-0004.1.

Hunt, K. M. R. and Menon, A., 2020, "The 2018 Kerala floods : a climate change perspective", *Clim. Dyn*., **54**. doi : 10.1007/s00382-020-05123-7.

Janjić, Z. I., 1994, "The Step-Mountain Eta Coordinate Model : Further Developments of the Convection, Viscous Sublayer and Turbulence Closure Schemes", *Mon. Wea. Rev*., **122**. doi : 10.1175/1520-0493(1994)122<0927:TSMECM>2.0.CO;2.

John, S. K., 2004, "The Kain-Fritsch Convective Parameterization: An Update", *J. Appl. Meteorol*., **43**. 170-181. doi : 10.1175/1520-0450(2004)043<0170:TKCPAU>2.0.CO;2.

Joseph, Susmitha, Sahai, Atul Kumar, Sharmila, S., Abhilash, S., Borah, Nabanita, Chattopadhyay, R., Pillai, Prasanth A., Rajeevan, M. and Kumar, Arun, 2015, "North Indian heavy rainfall event during June 2013 : diagnostics and extended range prediction", *Clim. Dyn*., **44**, 2049-2065. doi : 10.1007/s00382-014-2291-5.

Kain, J. S. and Fritsch, J. M., 1990, "A One-Dimensional Entraining/Detraining Plume Model and Its Application in Convective Parameterization", *J. Atmos. Sci*., **47**. doi : 10.1175/1520-0469(1990)047<2784:AODEPM>2.0.CO;2.

Kain, J. S. and Fritsch, J. M., 1992, "The role of the convective 'trigger function' in numerical forecasts of mesoscale convective systems", *Meteorol. Atmos. Phys.*, **49**. doi : 10.1007/BF01025402.

Kain, J. S., 2004, "The Kain-Fritsch Convective Parameterization : An Update", *J. Appl. Meteorol*., **43**. doi : 10.1175/1520-0450(2004)043<0170:TKCPAU>2.0.CO;2.

Kedia, S., Vellore, R. K., Islam, S. and Kaginalkar, A., 2019, "A study of Himalayan extreme rainfall events using WRF-Chem", *Meteorol. Atmos. Phys*., **131**, 1133-1143. doi : 10.1007/s00703-018-0626-1.

Lopez, P., 2007, "Cloud and Precipitation Parameterizations in Modeling and Variational Data Assimilation : A Review", *J. Atmos. Sci*., **64**. doi : 10.1175/2006JAS2030.1.

McKee, N., Chuang, H. and Wolff, J., 2019, Users' Guide for the NCEP Unified Post Processor (UPP) Version 4.

Mitra, A. K., Bohra, A. K., Rajeevan, M. N. and Krishnamurti, T. N., 2009, "Daily Indian Precipitation Analysis Formed from a Merge of Rain-Gauge Data with the TRMM TMPA Satellite-Derived Rainfall Estimates", *J. Meteorol. Soc. Japan*., **87A**, 265-279. doi : 10.2151/jmsj.87a.265.

Mlawer, Eli J., Taubman, Steven J., Brown, Patrick D., Iacono, Michael J. and Clough, Shepard A., 1997, "Radiative transfer for inhomogeneous atmospheres : RRTM, a validated correlated-k model for the longwave", *J. Geophys. Res*., **102**, 16,663-16,682. doi : 10.1029/97JD00237.

Nandargi, S., Gaur, A. and Mulye, S. S., 2016, "Hydrological analysis of extreme rainfall events and severe rainstorms over Uttarakhand, India", *Hydrol. Sci. J*., **61**, 2145-2163. doi : 10.1080/02626667.2015.1085990

Osuri, Krishna K., Mohanty, U. C., Routray, A., Kulkarni, Makarand A. and Mohapatra, M., 2012, "Customization of WRF-ARW model with physical parameterization schemes for the simulation of tropical cyclones over North Indian Ocean", *Nat. Hazards*, **63**, 1337-1359. doi: 10.1007/s11069-011-9862-0

Pai, D. S., Rajeevan, M., Sreejith, O. P., Mukhopadhyay, B. and Satbha, N. S., 2014, "Development of a new high spatial resolution (0.25° × 0.25°) long period (1901-2010) daily gridded rainfall data set over India and its comparison with existing data sets over the region", *MAUSAM*, **1**, 1-18.

Peatier, S., 2017, "Prediction of the Mumbai and the Mount Abu Extreme Events during the 2017 Monsoon Season in the IITM-MME and the S2S models".

Rajeevan, M., Kesarkar, A., Thampi, S. B., Rao, T. N., Radhakrishna, B. and Rajasekhar, M., 2010, "Sensitivity of WRF cloud microphysics to simulations of a severe thunderstorm event over Southeast India", *Ann. Geophys.*, **28**, 603-619. doi : 10.5194/ angeo-28-603-2010

Randall, D. A., 1989, "Cloud parameterization for climate modeling: Status and prospects", *Atmos. Res*., **23**, 345-361. doi : https:// doi.org/10.1016/0169-8095(89)90025-2.

Ray, Kamaljit, Pandey, Prabha, Pandey, Chhavi Pant, Dimri, A. P. and Kishore, K., 2019, "On the recent floods in India", *Curr. Sci*., **117**, 204-218.

Singh, D., Tsiang, M., Rajaratnam, B. and Diffenbaugh, N. S., 2014, "Observed changes in extreme wet and dry spells during the South Asian summer monsoon season", *Nat. Clim. Chang*., **4**, 456-461. doi : 10.1038/nclimate2208.

Skamarock, William C., Klemp, Joseph B., Dudhia, Jimy, Gill, David O., Barker, Dale M., Duda, Michael G., Huang, Xiang-Yu, Wang, Wei and Powers, Jordan G., 2019, "A Description of the Advanced Research WRF Model Version 4",

Stensrud, D. J., Bao, J. W. and Warner, T. T., 2000, "Using Initial Condition and Model Physics Perturbations in Short-Range Ensemble Simulations of Mesoscale Convective Systems", *Mon. Wea. Rev*., **128**, 2077-2107. doi : 10.1175/1520-0493(2000)128<2077:UICAMP>2.0.CO;2

Stensrud, D. J., Coniglio, M. C., Knopfmeier, K. H. and Clark, A. J., 2015, "NUMERICAL MODELS | Model Physics Parameterization", Encycl. Atmos. Sci., Second Ed 167-180. doi : 10.1016/B978-0-12-382225-3.00493-X.

Suhas, E., Zhang, G. J., 2014, "Evaluation of Trigger Functions for Convective Parameterization Schemes Using Observations", *J. Clim.*, **27**. doi : 10.1175/JCLI-D-13-00718.1.

Sundqvist, H., 1978, "A parameterization scheme for non-convective condensation including prediction of cloud water content", *Q. J. R. Meteorol. Soc*., **104**. doi : 10.1002/qj.49710444110.

Tahir, Khan Muhammad, Yin, Yan, Wang, Yong, Babar, Zaheer A. and Yan, Dong, 2015, "Impact Assessment of Orography on the Extreme Precipitation Event of July 2010 over Pakistan : A Numerical Study", *Adv. Meteorol*., 2015. doi : 10.1155/2015/510417.

Tiedtke, M., 1989, "A Comprehensive Mass Flux Scheme for Cumulus Parameterization in Large-Scale Models", *Mon. Wea. Rev*., **117**. doi : 10.1175/1520-0493(1989)117<1779:ACMFSF>2.0.CO;2.

Xu, Z. and Yang, Z. L., 2012, "An improved dynamical downscaling method with GCM bias corrections and its validation with 30 years of climate simulations", *J. Clim*., **25**, 6271-6286. doi : 10.1175/JCLI-D-12-00005.1.

Xue, Yongkang, Janjic, Zavisa, Dudhia, Jimy, Vasic, Ratko and Sales, Fernando De, 2014, "A review on regional dynamical downscaling in intraseasonal to seasonal simulation/prediction and major factors that affect downscaling ability", *Atmos. Res*., **147-148**, 68-85.

Yang, Linyun, Wang, Shuyu, Tang, Jianping, Niu, Xiaorui and Fu, Congbin, 2019, "Evaluation of the effects of a multiphysics ensemble on the simulation of an extremely hot summer in 2003 over the CORDEX-EA-II region", *Int. J. Climatol*., **39**, 3413-3430. doi : https://doi.org/10.1002/joc.6028.

Zhang, C. and Chou, M. D., 1999, "Variability of Water Vapor, Infrared Radiative Cooling and Atmospheric Instability for Deep Convection in the Equatorial Western Pacific", *J. Atmos. Sci*., **56**. doi : 10.1175/1520-0469(1999)056<0711:VOWVIR> 2.0.CO;2.

Zhang, C. and Wang, Y., 2017, "Projected Future Changes of Tropical Cyclone Activity over the Western North and South Pacific in a 20-km-Mesh Regional Climate Model", *J. Clim*., **30**, 5923-5941. doi : 10.1175/JCLI-D-16-0597.1.

Zhang, S. 2011, "A Study of Impacts of Coupled Model Initial Shocks and State-Parameter Optimization on Climate Predictions Using a Simple Pycnocline Prediction Model", *J. Clim*., **24**, 6210-6226. doi : 10.1175/JCLI-D-10-05003.1.